LIPOPROTEIN RECEPTOR SR-B1 DEFICIENCY ENHANCES ADIPOSE TISSUE INFLAMMATION AND REDUCES SUSCEPTIBILITY TO HEPATIC STEATOSIS DURING DIET-INDUCED OBESITY IN MICE

Thesis submitted in compliance with the requirements

to obtain a degree of Master of Health Sciences Research

By

Katherine Solange Rivera Vega

Academic Tutor:

Dr. Attilio Rigotti

Academic Co-Tutor:

Dr. Marcelo Andia

August 2020

INDEX OF CONTENTS

1. INDEX OF FIGURES AND TABLES

2. LIST OF ABBREVIATIONS

ALT: alanine transaminase

ApoA-I: apolipoprotein A-I

Apob: apolipoprotein B

AUC: area under the curve

BMI: body mass index

CLS: crown-like structures

Cpt1: carnitine palmitoyltransferase 1

CVD: cardiovascular disease

Dgat2: diacylglycerol o-acyltransferase 2

ELISA: enzyme-linked immunosorbent assay

eWAT: epididimal WAT

FA: fatty acids

Fasn: fatty acid synthase

FFA: free FA

FPLC: fast protein liquid chromatography

Gapdh: glyceraldehyde-3-phosphate dehydrogenase

GC-MS: gas chromatography with mass spectrometer

GGT: gamma-glutamyltransferase

H&E: hematoxylin-eosin

HDL: high-density lipoprotein

HDL-C: HDL cholesterol

HFD: high fat diet

HOMA-IR: homestatic model of assessment for IR

IL-10: interleukin 10

IR: insulin resistance

LDL: low-density lipoprotein

Ldlr: LDL receptor

LPL: lipoprotein lipase

Lrp1: low-density lipoprotein receptor-related protein 1

Mgat1: monoacylglycerol acyltransferase 1

Mttp: microsomal triglyceride transfer protein

MAFLD: metabolic (dysfunction) associated fatty liver disease

MUFA: monounsaturated FA

NAFLD: non-alcoholic fatty liver disease

NASH: non-alcoholic steatohepatitis

PCA: principal components analysis

PPARα: Peroxisome proliferator-activated receptor α

PPARγ: peroxisome proliferator-activated receptor γ

PUFA: polyunsaturated FA

RCT: reverse cholesterol transport

RT-PCR: reverse transcription & polymerase chain reaction

S1P: sphingosine 1 phosphate

Scd1: stearoyl-CoA desaturase 1

SFA: saturated FA

SR-B1: scavenger receptor class B type 1

Srebp1c: sterol regulatory element binding protein 1c

TG: triglycerides

TNF-α: tumor necrosis factor-α

VLDL: very-low-density lipoproteins

WAT: white adipose tissue

WT: wild-type

3. ABSTRACT

Obesity is a worldwide epidemic associated with excessive lipid accumulation in adipose and non-adipose tissues, including the liver, an early feature in the development of non-alcoholic fatty liver disease (NAFLD). Several studies have linked NAFLD with a deranged high-density lipoprotein (HDL) metabolism. Scavenger receptor class B type 1 (SR-B1) is the major membrane HDL receptor and is involved in reverse cholesterol, but its role in obesity and NAFLD development is unclear. The aim of this thesis was to determine the effects of SR-B1 deficiency on plasma metabolic parameters and fat deposition in adipose tissue and liver during obesity.

Male SR-B1 knock-out (SR-B1$^{-/-}$) mice and wild-type (WT) littermates were fed for 12 weeks with a high-fat diet (HFD) to induce obesity. At the end of the intervention SR-B1$^{-/-}$ mice fed a HFD exhibited significantly increased levels of plasma total cholesterol, triglycerides (TG) and TNF-α, in association with hypertrophied adipocytes and macrophage-containing crown-like structures (CLS) in adipose tissue, compared to WT obese mice. Remarkably, obese SR-B1$^{-/-}$ mice exhibited attenuated liver TG content, dysregulation in hepatic gene expression profile, increased hepatic TG secretion, and altered hepatic fatty acid (FA) composition, compared to WT mice.

These results provide the basis for further elucidation of SR-B1 role in obesity and fatty liver disease, two major worldwide public health issues that increase the risk of advanced chronic disease and mortality in the general population.

4. INTRODUCTION

Obesity is a multifactorial syndrome and the major risk factor for a variety of cardiometabolic diseases [1]. This condition, characterized by abnormal or excess fat accumulation, promotes a chronic inflammatory state and atherogenic dyslipidemia, which is strongly associated with insulin resistance (IR) and diabetes, increased cardiovascular disease (CVD) incidence and mortality risk in the general population [2].

During obesity, alterations in white adipose tissue (WAT) can promote lipid accumulation in the liver, leading to intracellular lipid droplet formation, a condition known as hepatic steatosis [3]. In several pathological conditions, these lipid droplets may expand and potentially interfere with essential hepatocellular functions [4]. This alteration is a hallmark feature of non-alcoholic fatty liver disease (NAFLD), the most prevalent liver disease worldwide that results in a major impact on the health and economic burden [5].

Although obesity is intimately associated with liver fat accumulation and its comorbidities, some observations have documented that not all patients with obesity develop metabolic complications, supporting the idea that genetic variants could predispose a subset of obese subjects to increased risk of chronic abnormalities and death [5–7]. Indeed, special attention in lipid transport-related proteins on development of metabolic complications induced by obesity could help to understand this wide variety of obesity-related phenotypes [8]. Interestingly, circulating high-density lipoprotein cholesterol (HDL-C) and triglyceride (TG) levels are altered in obese subjects with fatty liver disease [9,10]. In addition, recent observations have shown that impaired HDL-C efflux capacity is associated with subclinical atherosclerosis in NAFLD patients, which contributes to increased CVD risk [11].

Scavenger receptor class B type 1 (SR-B1) is a key membrane receptor that modulates the bidirectional flux of lipids between lipoproteins and cells in different tissues [12]. As a hallmark of lipoprotein metabolism, hepatic SR-B1 mediates HDL lipid delivery through reverse cholesterol transport (RCT), playing a vital role in against atherosclerosis [13,14]. However, the specific role of SR-B1 during obesity and progression of its comorbidities is still not fully understood.

Studies using 3T3-L1 adipocytes have shown that lipogenic stimulation promoted the mobilization of SR-B1 to the plasma membrane [15,16]. Besides, SR-B1 protein expression was down-regulated by inflammatory tumor necrosis factor-α (TNF-α) exposure in partially differentiated adipocytes [17]. In addition, the expression of SR-B1 in hepatocytes was modulated by peroxisome proliferator-activated receptor γ (PPARγ), a crucial regulator of lipogenic pathways [18]. Remarkably, a recent study showed that SR-B1 modulation by overexpression or siRNA-mediated knockdown regulates fatty acid (FA) uptake in cells [19]. Taken together, these findings strongly suggest that SR-B1 may play a crucial role in metabolic environment maintenance and lipid deposition during obesity.

5. HYPOTHESIS

SR-B1 expression modulates the metabolic and inflammatory phenotype of obese mice through the regulation of lipid deposition within adipocytes and hepatocytes.

6. OBJECTIVES

General

Determine the effects of SR-B1 deficiency on plasma metabolic parameters and fat deposition in adipose tissue and liver during obesity.

Specifics

1- Analyze the levels of lipids and inflammatory markers in plasma of obese SR-B1-deficient mice.

2- Assess the impact of SR-B1 deficiency on adipocyte morphology and adipose tissue inflammation.

3- Study whether the expression of SR-B1 contributes to the development of hepatic steatosis during obesity.

4- Characterize the markers of the main pathways involved in lipid deposition in the liver of SR-B1-deficient obese mice.

7. METHODS

7.1. Animals and diet

Mice with a targeted mutation in the SR-B1 gene locus on a C57BL/6J:129 mixed background (B6.129S2-Scarb1tm1Kri) were originally obtained from Dr. Monty Krieger (Massachusetts Institute of Technology, Cambridge, MA, USA) and maintained in the animal facility of the School of Medicine, Pontificia Universidad Católica de Chile at 25°C and 12 h light:dark cycling. For diet-induced obesity, 8-week-old homozygous SR-B1 knock-out (SR-B1$^{-/-}$, n=14) male mice and wild-type (WT, n=12) littermates were fed for 12 weeks with a high-fat diet (HFD) (60% kcal from fat; 58Y1 TestDiet, St. Louis, MO, USA) in three independent sets. Body weight and food intake were weekly assessed during the duration of the study and none important adverse events were observed. All procedures were performed following the Guide for the Care and Use of Laboratory Animals (copyright 1996, National Academy of Science) published by National Research Council (NRC) and approved by the Ethics and Animal Welfare Committee from the School of Medicine of the Pontificia Universidad Católica de Chile (Protocol #14-036).

7.2. Tissue sampling

After 12 weeks of dietary intervention, WT and SR-B1$^{-/-}$ obese animals were euthanized with a mixture of ketamine:xylazine (150:10 mg/kg, intraperitoneally) after overnight fasting. Blood was collected by cardiac puncture. Plasma was obtained by low-speed centrifugation of blood and kept at -80°C until further analysis. Epididymal WAT (eWAT) and liver samples were removed, weighed, and flash frozen in liquid nitrogen or processed for histological analyses by light microscopy and immunohistochemistry.

7.3. Biochemical analyses

Plasma or frozen tissues were used for biochemical analyses. Plasma total cholesterol levels were quantified through an enzymatic method described previously [20]. Plasma TG and free FA (FFA) concentrations were measured through enzymatic assays with commercial kits, following the manufacturers' recommendations (Sigma-Aldrich, St. Louis, MO, USA). Plasma concentrations of TNF-α and interleukin 10 (IL-10) were determined using enzyme-linked immunosorbent assay (ELISA) kits (R&D Systems, Minneapolis, MN, USA). Plasma levels of leptin and adiponectin were also determined using ELISA kits (Sigma-Aldrich, St. Louis, MO, USA). Total lipids from liver samples were extracted using a chloroform/methanol solution (2:1, vol/vol), as previously described [21], and total TG and cholesterol content were analyzed by the enzymatic tests used for plasma. Lipoprotein cholesterol levels were quantified in fast protein liquid chromatography (FPLC)-fractionated plasma samples as described previously [20]. Plasma glucose-to-insulin ratio and homestatic model of assessment for insulin resistance (IR) (HOMA-IR; fasting plasma insulin (μU/ml) × fasting glucose (mmol/L)/22.5) were also calculated. Plasma levels of liver enzymes [alanine transaminase (ALT) and gamma-glutamyltransferase (GGT)] were measured with a commercial kit through a UV method, according to the manufacturer's instructions (HUMAN Diagnostics Worldwide, Wiesbaden, Denmark).

7.4. Histological analyses

For standard histology, eWAT and liver tissue samples were fixed overnight in 10% formalin at 4°C, then dehydrated, cleared, and paraffin-embedded. Ten-micrometer sections from formalin-fixed paraffin-embedded eWAT and liver samples were mounted and stained with hematoxylin and eosin (H&E) solution. All stained slides were examined with a Nikon Eclipse E200 light microscope and photographed with a Nikon DS-Fi1 camera. Representative images from each tissue (4–5 per animal) were taken and

adipocyte and liver lipid droplets areas were blind measured for at least 100 individual cells per mice using Image J software (National Institutes of Health, Bethesda, MD, USA).

For immunohistochemistry, dewaxed 3 µm serial sections of paraffin-embedded eWAT were treated with 3% hydrogen peroxide to inactivate endogenous peroxidases and then macrophage cell infiltration of the adipose tissue was characterized using anti-MAC-2 (1:100; Cedarlane Laboratories, Paletta Court, Burlington, Ontario, Canada), as previously described [22]. Biotinylated HRP-conjugated secondary antibodies were goat anti-mouse IgG (H+L) (Molecular Probes, Life Technologies, Thermo Fisher Scientific, Waltham, MA, USA). The histochemical reaction was performed using 3,3′-diaminobenzidine as a substrate (Sigma-Aldrich, St. Louis, MO). Sections were counterstained with hematoxylin. Tissue sections were observed and macrophage-containing crown-like structure (CLS) density was obtained by counting the total number of CLS in each section compared with the total number of adipocytes and expressed as CLS number/1,000 adipocytes.

7.5. Quantitative Real-Time PCR assay

Total RNA from livers was extracted using Trizol Reagent (Invitrogen Corporation, Carlsbad, CA, USA) following manufacturer instructions. Aliquots of 1-2 µg of RNA from each tissue sample were reverse-transcribed to cDNA by a high-capacity cDNA reverse transcription kit (Applied Biosystems, Foster City, CA, USA). The reverse transcription polymerase chain reaction (RT-PCR) was performed by QuantiTest SYBR Green PCR kit (Applied Biosystems, Foster City, CA, USA) using the ABI 7300 sequence detection system (Applied Biosystems, Foster City, CA, USA) according to the protocols provided by the manufacturer. The specific mRNA levels were quantified and normalized to those of glyceraldehyde-3-phosphate dehydrogenase (Gapdh) using the mathematical model previously described [23]. For primer list and sequences, see **Table 1**.

Table 1. RT-PCR primers sequences for mRNA analysis

Gene	Forward primer	Reverse primer
Gapdh	TGCGACTTCAACAGCAACTCCCAC	TTGCTCAGTGTCCTTGCTGGGG
Lrp1	TGGGTCTCCCGAAATCTGTT	ACCACCGCATTCTTGAAGGA
Ldlr	AGGCTGTGGGCTCCATAGG	TGCGGTCCAGGGTCATCT
Srebp1c	GGAGCCATGGATTGCACATT	GGCCCGGGAAGTCACTGT
Scd1	CCGGAGACCCCTTAGATCGA	TAGCCTGTAAAAGATTTCTGCAAACC
Fasn	GCTGCGGAAACTTCAGGAAAT	AGAGACGTGTCACTCCTGGACTT
Mgat1	CTGGTTCTGTTTCCCGTTGT	TGGGTCAAGGCCATCTTAAC
Dgat2	CCGCAAAGGCTTTGTGAAG	GGAATAAGTGGGAACCAGATCA
Pparα	ACAAGGCCTCAGGGTACCA	GCCGAAAGAAGCCCTTACAG
Cpt1	CACCAACGGGCTCATCTTCTA	CAAAATGACCTAGCCTTCTATCGAA
Pparγ	GCAGAGACAAATGTGCTTCG	TCTGGGGTCAGAGGAAGAGA
Apob	CGTGGGCTCCAGCATTCTA	TCACCAGTCATTTCTGCCTTTG
Mttp	CCTACCAGGCCCAACAAGAC	CGCTCAATTTTGCATGTATCC

Gapdh, Glyceraldehyde-3-phosphate dehydrogenase; *Lrp1*, Low-density lipoprotein receptor related protein; *Ldlr*, Low-density lipoprotein receptor; *Srebp1c*, Sterol regulatory element binding protein 1c; *Scd1*, Stearoyl-coA desaturase 1rp1; *Fasn*, Fatty acid synthase; *Mgat1*, Monoacylglycerol acyltransferase 1; *Dgat2*, Diacylglycerol o-acyltransferase 2; *Ppar*□, Peroxisome proliferator-activated receptor □; *Cpt1*, Carnitine palmitoyltransferase 1; *Ppar*□, Peroxisome proliferator-activated receptor □; *Apob*, Apolipoprotein b; *Mttp*, Microsomal triglyceride transfer protein.

7.6. Western blot

Liver samples were disrupted in homogenization buffer with protease inhibitors and the homogenates were used for protein quantification by Bio-Rad Protein Assay (Bio-Rad Laboratories, Hercules, CA, USA). Western blot analysis of PPARγ protein in the liver was performed using 50 µg of protein/sample. Proteins were size-fractionated in 12% SDS-PAGE gels and transferred onto PVDF membranes. For protein detection, specific primary and secondary antibodies were used as follows. The membrane was incubated with rabbit polyclonal antibody to PPARγ (Cell Signalling Technology, Inc., London, United Kingdom) overnight at 4°C. PPARγ protein expression was normalized to ε-COP using a rabbit polyclonal antibody obtained from Dr. Monty Krieger (Massachusetts Institute of Technology, Cambridge, MA, USA). After incubation with the primary antibody, the membrane was washed and incubated with peroxidase-conjugated secondary antibodies (Invitrogen, Carlsbad, CA, USA), and the bound antibody was visualized with the ECL kit (Amersham, Buckinghamshire, United Kingdom) and X-Omat S film (Eastman Kodak Co., Rochester, NY, USA).

7.7. Hepatic triglyceride secretion

To measure hepatic TG production, mice fed on a HFD for 12 weeks were fasted for 4 hr to prevent the intestinal secretion of chylomicrons. Animals were injected with Tyloxapol (Sigma-Aldrich, St. Louis, MO), a lipoprotein lipase inhibitor, at 500 mg/kg intravenously in saline, as previously shown to be optimal in mice [24]. Immediately before injection and at 1 hr post-injection, blood samples were drawn in heparinized capillary tubes and plasma was prepared and fractionated by FPLC using a Superose-6 10/300 GL column (GE Healthcare Life Sciences, Marlborough, MA, USA), as previously described [20].

Lipoprotein fractions eluted according to their particle size were recovered and TG concentrations were determined.

7.8. Lipid fatty acid profile analysis

Lipids were extracted from livers using a chloroform/methanol solution (2:1, vol/vol), as previously described [21], and subjected to esterification for analytical stability. Total FA were analyzed using gas chromatography–mass spectrometry (GC-MS) (PerkinElmer, Clarus 680, Waltham, MA, USA) equipped with HP-Innowax capillary column (length 25 meters, 0.2 mm internal diameter, 0.2 mm film). Data register was in SCAN mode and peak integration was obtained by the TurboMass Training 2016 PRO software. FA peaks were identified based on comparing retention times with external standards, and mass was calculated according to the integration area of corresponding peaks. FA composition was defined as the percentage of individual fatty acids relative to total content, as previously detailed [25].

7.9. Stadistical analyses

Statistical analyses were performed using GraphPad Prism 8.0.1 (GraphPad Software, San Diego, CA, USA). The normality of data was determined with the Kolmogorov–Smirnov test. Unpaired Student's t-test was used to assess whether the means of two normally distributed groups differed significantly, and Mann Whitney U-test as its non-parametric counterpart. Two-way ANOVA analysis with repeated measures was also used in some data evaluation with Bonferroni's multiple comparisons post-hoc test. Tests were two-tailed and differences were considered significant when $p < 0.05$, where n indicates the sample size. R was used for principal component analysis (PCA).

8. RESULTS

8.1. SR-B1 expression influences plasma lipid and cytokine levels in HDF-fed mice

We used a high-calorie fat-based diet to evaluate a putative role of SR-B1 deficiency on the metabolic phenotype and the potential mechanisms involved during diet-induced obesity in mice. As expected, animals fed a HFD for 12 weeks turned significantly obese as indicated by higher body weights, compared to baseline ($p < 0.0001$) (**Fig. 1A**). However, the body weight gain and the average food intake were similar between SR-B1$^{-/-}$ and WT groups (**Fig. 1A-B**).

Next, we performed biochemical measurements to investigate whether SR-B1 deficiency affected key plasma parameters of obesity-associated metabolic dysfunction. Higher levels of total plasma cholesterol (+107%, $p < 0.0001$) were found in HFD-fed SR-B1$^{-/-}$ mice than in obese WT mice (**Fig. 1C**). Consistently, the lipoprotein profile showed that plasma cholesterol levels were associated with HDL-C accumulation in SR-B1$^{-/-}$ mice (**Fig. 1D**), most likely due to decreased selective HDL cholesterol uptake previously reported in chow-fed SR-B1 knock-out animals [26].

Surprisingly, the absence of SR-B1 in obese mice also caused a significant increase in circulating TG levels (+50%, $p < 0.01$), while plasma FFA levels were similar ($p > 0.05$) in comparison with WT mice (**Fig. 1E-F**). Furthermore, we found that TNF-α levels were also significantly higher in obese SR-B1$^{-/-}$ mice than in WT (+32%, $p < 0.0001$) (**Fig. 1G**). A trend to lower plasma IL-10 levels was also observed in obese SR-B1-deficient mice vs. obese WT ($p = 0.0749$) (**Fig. 1H**). These data suggest that SR-B1 deficiency in HFD-fed mice associated with inflammatory dyslipidemia.

Interestingly, obese SR-B1-deficient mice showed impaired insulin sensitivity as indicated by higher HOMA-IR compared to WT (**Fig. 1l**), suggesting that SR-B1 may be involved directly or indirectly in obesity-induced IR.

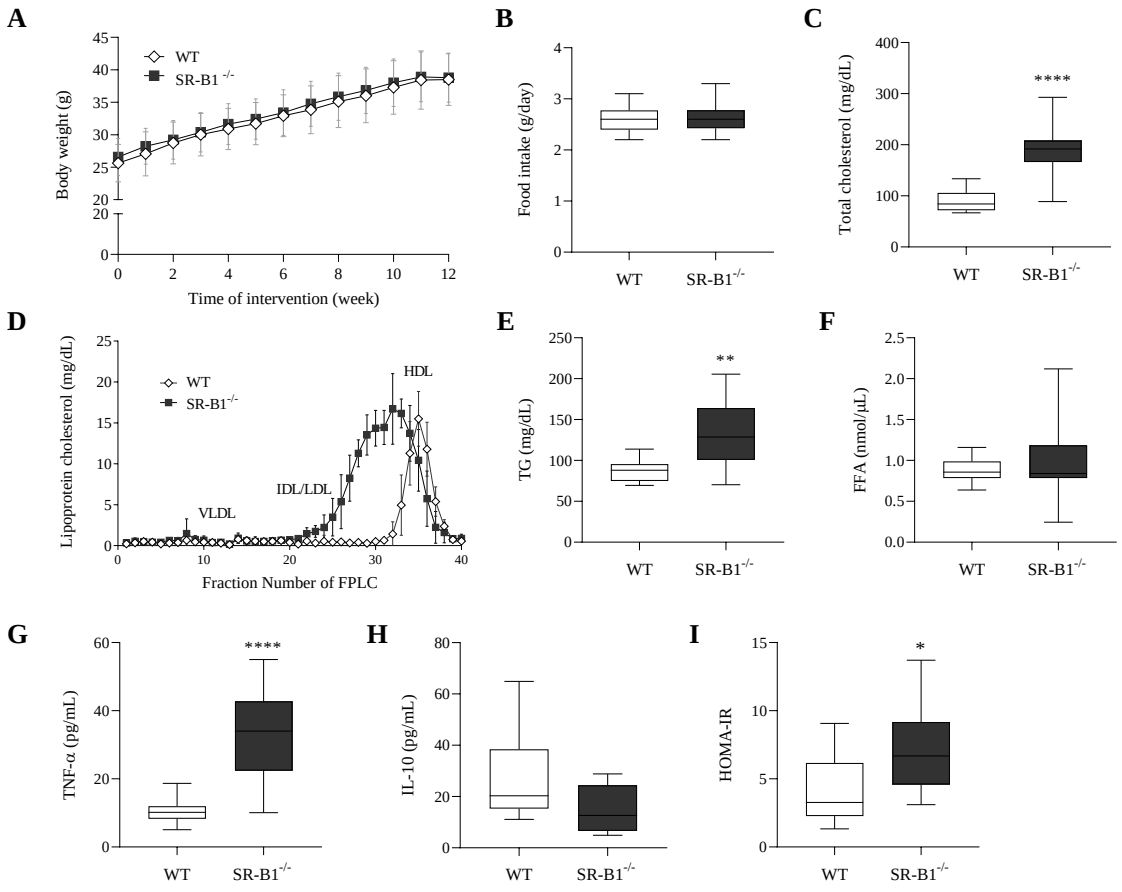

Fig 1. Body weight, food intake, and plasma metabolic/inflammatory markers in SR-B1$^{-/-}$ mice fed on a HFD for 12 weeks. (A) Body weight gain and **(B)** food intake for WT (n=12) and SR-B1$^{-/-}$ (n=14) mice. Plasma **(C)** total cholesterol, **(D)** lipoprotein cholesterol, **(E)** TG, **(F)** FFA, **(G)** TNF-α, and **(H)** IL-10 levels. **(I)** HOMA-IR for WT (n=12) and SR-B1$^{-/-}$ (n=14) mice. Data are presented as mean ± SD or shown in box plots. ** $p < 0.01$; **** $p < 0.001$ vs. WT mice.

8.2. Absence of SR-B1 promotes inflammatory hypertrophy of white adipocytes in obese mice

Adipose tissue is the main organ that stores the excess of energy intake as TG. It is well known that HFD intake increases adipocyte size and adipose tissue mass, contributing to adipose tissue inflammation and its associated metabolic abnormalities [27,28].

To investigate whether adipose morphology was changed in animals lacking SR-B1 under obesity, we examined the average adipocyte size in obese mice. Surprisingly, we found that SR-B1$^{-/-}$ obese animals had a shift towards bigger fat cells, compared to WT littermates ($p < 0.0001$) (**Fig. 2A-C**). Furthermore, in order to assess the inflammatory status of the adipose tissue in obese SR-B1$^{-/-}$ mice, we performed immunostaining analysis of macrophages using the anti-MAC-2 (Galectin-3) antibody [22]. In association with adipocyte hypertrophy, HFD-fed SR-B1$^{-/-}$ mice presented a detrimental effect on macrophage-containing CLS (**Fig. 2D**), exhibiting a significant increase in the density of CLS in adipose tissue in comparison with HFD-fed WT mice (+194%, $p < 0.01$) (**Fig. 2E**).

Adipocytes are the source of several hormones that regulate whole-body metabolism, including leptin and adiponectin [29]. However, the expression of SR-B1 did not significantly modify plasma adiponectin (**Fig. 2F**) or leptin (**Fig. 2G**) levels compared to WT mice after consumption of the HFD diet ($p > 0.05$).

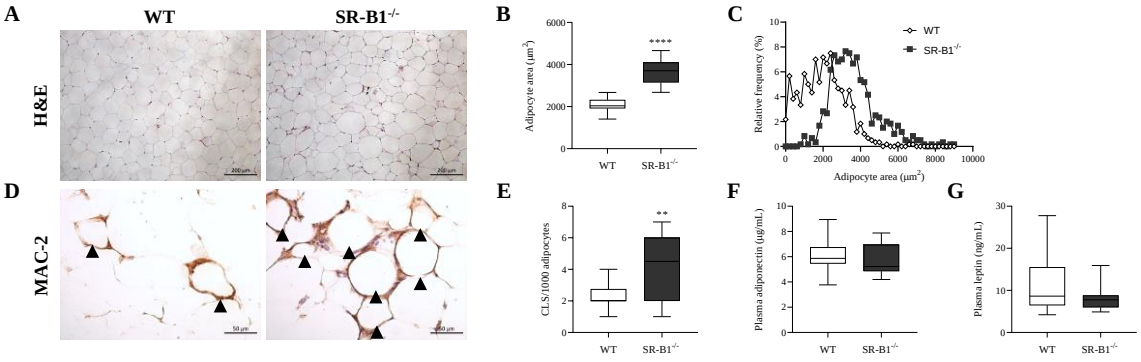

Fig 2. Adipose tissue histological analysis and plasma adipokine levels in SR-B1$^{-/-}$ mice fed on a HFD for 12 weeks. (A) Representative H&E-stained sections of eWAT. **(B)** Mean adipocyte cross-sectional area for WT (n=11) and SR-B1$^{-/-}$ (n=14) mice. **(C)** The frequency distribution of adipocyte sizes for WT (n=12) and SR-B1$^{-/-}$ (n=14) mice. **(D)** Representative MAC-2 inmmunostained cross sections of eWAT showing CLS. **(E)** Quantitative assessment of CLS per 1,000 adipocytes for WT (n=12) and SR-B1$^{-/-}$ (n=14) mice. Plasma **(F)** adiponectin and **(G)** leptin levels for WT (n=12) and SR-B1$^{-/-}$ (n=14) mice. Data are shown in box plots. ** $p < 0.01$; **** $p < 0.001$ vs. WT mice.

8.3. Obese SR-B1-deficient exhibited marked decrease in hepatic steatosis

During obesity, pathological adipocyte enlargement in association with fat tissue immune cell infiltration leads to lipid accumulation in non-adipose tissue [27]. To explore the potential role of SR-B1 expression on the pathogenesis of NAFLD, we investigated its involvement in liver steatosis development in response to HFD intake in WT and SR-B1$^{-/-}$ mice. Surprisingly, livers from SR-B1 deficient animals showed normal size and weight but were less yellowish, suggesting attenuated fatty liver, compared to WT mice (**Fig. 3A**). Indeed, intrahepatic lipid droplet formation were evaluated by H&E staining supporting that obese SR-B1-deficient mice exhibited fewer lipid deposits (**Fig. 3B**) as well as decreased size in hepatocyte lipid droplets, compared with WT mice (-57%, $p < 0.0001$) (**Fig. 3C**).

As expected, biochemical measurements of total TG and cholesterol hepatic content showed that liver steatosis observed in WT obese mice was due to excess accumulation of TG rather than cholesterol (**Fig. 3D-E**). Specifically, HFD-fed SR-B1$^{-/-}$ mice had a significantly lower TG content (-52.6%, $p < 0.0001$) but similar levels of cholesterol ($p > 0.05$) compared to WT mice (**Fig. 3D-E**).

Despite the marked dependence of liver fat accumulation on SR-B1 expression, NAFLD-associated injury ALT and GGT enzymes in plasma samples showed no changes comparing SR-B1$^{-/-}$ and WT mice after HFD-intake for 12 weeks ($p > 0.05$) (**Fig. 3F-G**).

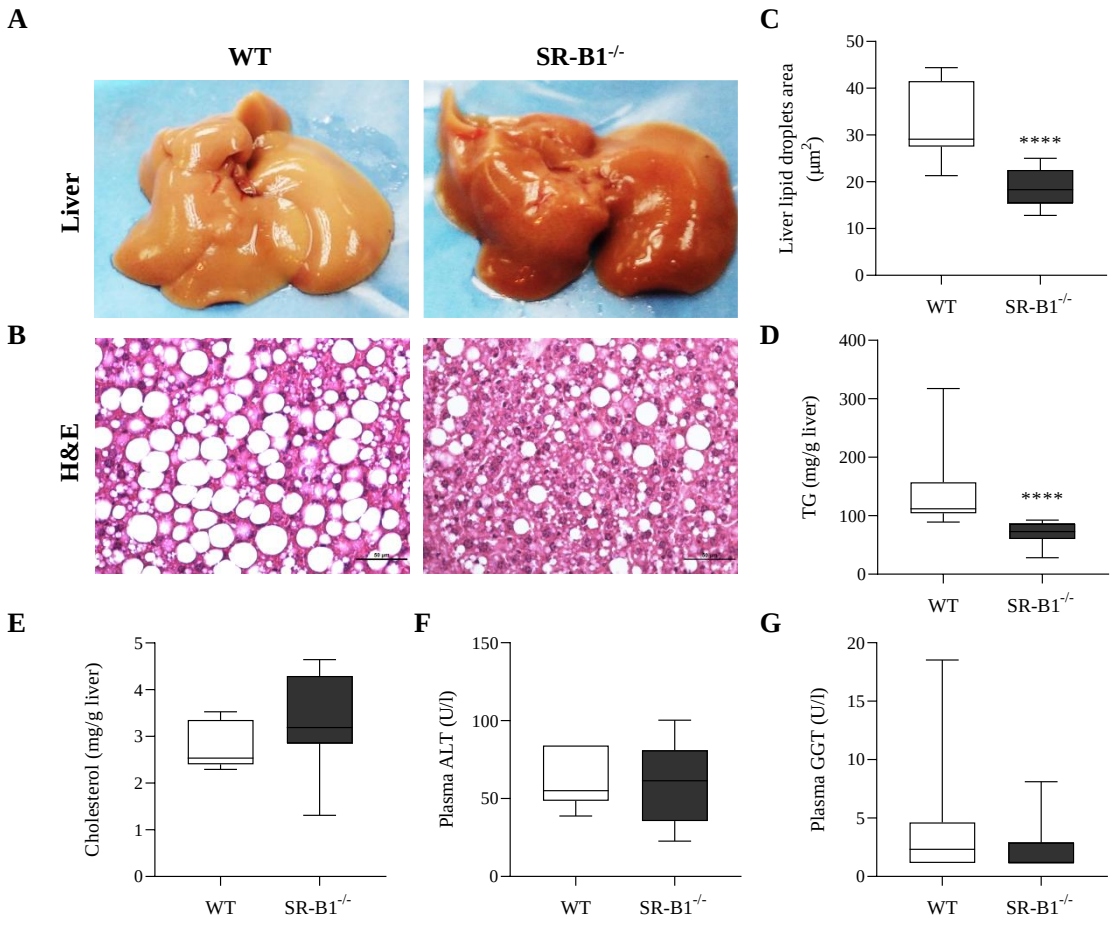

Fig 3. Liver tissue analysis and plasma enzyme levels in SR-B1$^{-/-}$ mice fed on a HFD for 12 weeks. Representative images of **(A)** livers and **(B)** H&E-stained liver sections obtained from HFD-fed mice. **(C)** Mean liver lipid droplet area for WT (n=12) and SR-B1$^{-/-}$ (n=14) mice. **(D)** Hepatic TG content for WT (n=12) and SR-B1$^{-/-}$ (n=14) mice. **(E)** Hepatic cholesterol content for WT (n=7) and SR-B1$^{-/-}$ (n=8) mice. Plasma **(F)** ALT and **(F)** GGT levels for WT (n=7) and SR-B1$^{-/-}$ (n=9) mice. Data shown in box plots. **** $p < 0.001$ vs. WT.

8.4. Effect of SR-B1-deficient on hepatic protein and gene expression during obesity

A delicate balance between anabolic and catabolic processes regulates the hepatic lipid metabolism [30]. Indeed, PPARs and their target genes modulate lipogenesis, lipid oxidation, and lipid accumulation in steatotic hepatocytes [31,32]. To delineate the mechanisms by which the absence of SR-B1 attenuated steatosis during obesity, we next examined the expression of key hepatic protein/genes involved in lipid uptake, biosynthesis, and catabolism.

Interestingly, in livers from obese mice, the absence of SR-B1 -compared with WT animals- was significantly associated with a decrease in PPARγ protein levels (**Fig. 4A**). In addition, consistent with western blot analysis, *Pparg* mRNA levels were down-regulated in HFD-fed SR-B1-deficient mice in comparison to WT mice (**Fig. 4B**). We did not observe any significant differences in genes regulating the uptake of lipoprotein, such as low-density lipoprotein receptor-related protein (*Lrp1*) and low-density lipoprotein receptor (*Ldlr*) ($p > 0.05$) (**Fig. 4B**). Also, mRNA levels of genes regulating FA and TG synthesis, such as sterol regulatory element-binding protein 1c (*Srebp1c*), stearoyl-CoA desaturase 1 (*Scd1*), fatty acid synthase (Fasn), monoacylglycerol acyltransferase 1 (*Mgat1*), and diacylglycerol o-acyltransferase 2 (*Dgat2*), did not show changes associated with SR-B1 expression ($p > 0.05$) (**Fig. 4B**). Interestingly, obese SR-B1-deficient mice expressed significantly higher levels of hepatic genes associated with β-oxidation, including peroxisome proliferator-activated receptor a (*Ppara*) and carnitine palmitoyltransferase 1 (*Cpt1*), compared to obese WT mice ($p < 0.05$) (**Fig. 4B**). Taken together, these data indicate that the impact of SR-B1 expression on fatty liver was due in part to modulated expression of PPARs and some of their target genes.

Remarkably, SR-B1-deficiency was also associated with an approximate 2-fold increase in hepatic levels of apolipoprotein b (*Apob*) mRNA after HFD intake compared to the WT group ($p < 0.05$) (**Fig. 4B**), while no differences were observed in the expression of microsomal triglyceride transfer protein (*Mttp*) ($p > 0.05$) (**Fig. 4A**), both keys determinants of hepatic VLDL assembly and secretion.

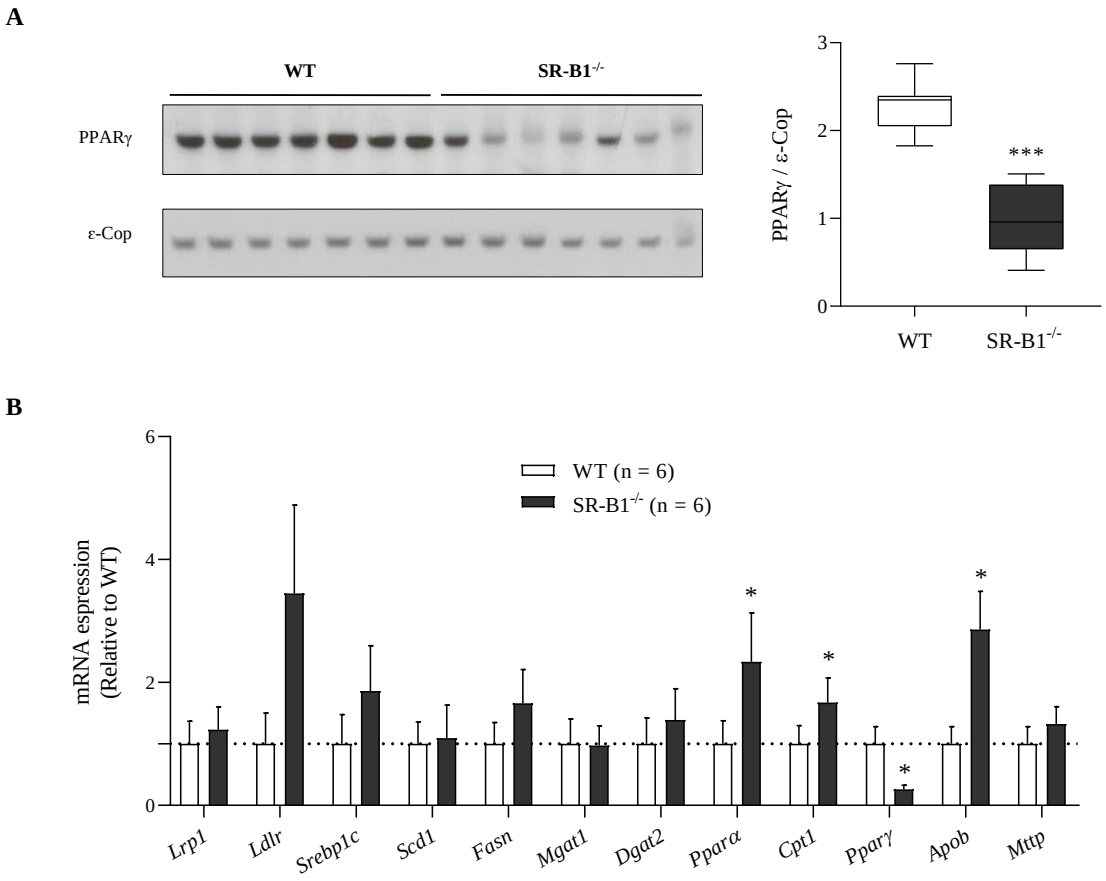

Fig 4. Hepatic protein and gene expression analyses in SR-B1$^{-/-}$ mice fed on a HFD for 12 weeks. (A) Immunoblotting analysis and quantitation of PPARγ protein level in total liver lysates for WT (n=7) and SR-B1$^{-/-}$ (n=7) mice. **(B)** Quantitative RT-PCR gene expression for WT (n=6) and SR-B1$^{-/-}$ (n=6) mice. Data are presented in box plots or shown as mean ± SD. * $p < 0.05$; *** $p < 0.001$ vs. WT mice.

8.5. SR-B1 deficiency increases VLDL-TG secretion in obese mice

During post-absorptive fasting conditions, very-low-density lipoproteins (VLDL) particles produced by the liver are the primary carriers of TG in plasma, which require apoB synthesis in the liver [33]. In order to determine if SR-B1 expression modulated hepatic and plasma TG levels after HFD feeding through changes in VLDL-TG secretion, we measured plasma accumulation of VLDL-TG after treatment with Tyloxapol, which acutely inhibits peripheral lipolysis of TG-rich lipoproteins.

As shown in **Fig. 5A**, HFD-fed SR-B1$^{-/-}$ mice pretreated with tyloxapol had significantly increased plasma TG levels and VLDL-TG secretion compared to WT obese mice. These results indicate that the absence of SR-B1 during obesity stimulates hepatic VLDL-TG secretion ($p < 0.0001$). In addition, analysis of the area under the curve (AUC) of TG levels in lipoprotein fractions revealed a significant increase (+266%, $p < 0.01$) in obese SR-B1-deficient vs. WT animals (**Fig. 5B**).

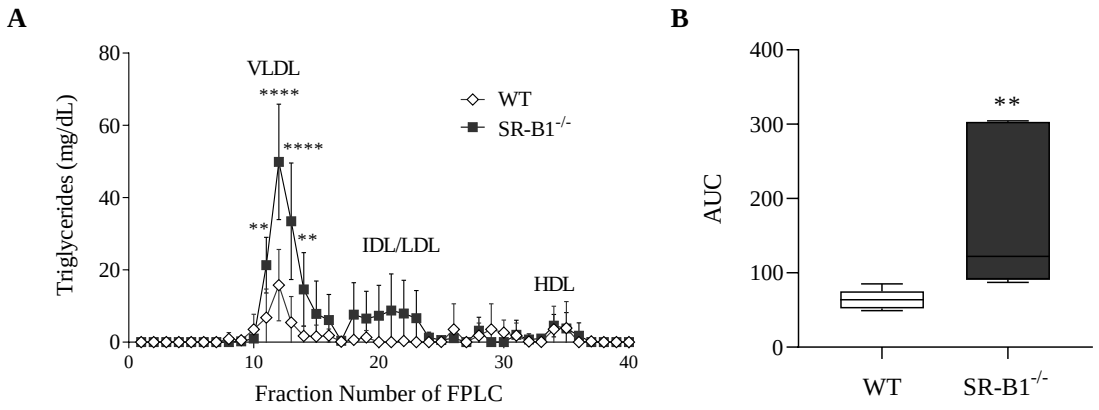

Fig 5. Hepatic VLDL-TG secretion analysis in SR-B1$^{-/-}$ mice fed an HFD for 12 weeks. **(A)** TG content in lipoprotein fractions and **(B)** AUC of chromatogram after Tyloxapol injection for WT (n=6) and SR-B1$^{-/-}$ (n=6) mice. Data are presented as mean ± SD or shown in box plots. ** $p < 0.01$; **** $p < 0.001$ vs. WT mice.

8.6. SR-B1-deficiency differentially affects hepatic FA composition in HFD-fed mice

Liver FA composition is closely related to the severity and progression of NAFLD [34]. Previous studies strongly suggest that β-oxidation plays a crucial role in regulating the FA profile [35].

Thus, in order to evaluate if SR-B1 expression modify the hepatic FA content during obesity, we compared liver FA composition in HFD-fed WT and SR-B1$^{-/-}$ mice. We identified eight main FA (C16:0, C16:1, C18:0, C18:1, C18:2, C20:4, C22:5, C22:6) that were considered in this analysis. SR-B1-deficient mice fed a HFD showed lower C18:1 (oleic acid) content compared to HFD-fed WT mice (34.8 ± 2.38 vs. 39.6 ± 1.64 %, $p < 0.01$) (**Fig. 6A**). Furthermore, FA were grouped and analyzed based on three main standard categories: saturated (SFA), monounsaturated (MUFA), and polyunsaturated FA (PUFA). **Fig. 6B** shows that the absence of SR-B1 in obese mice was associated with overall reduced liver MUFA content (36.9 ± 2.55 vs. 41.8 ± 1.55 %, $p < 0.01$), compared with WT obese mice. SFA and PUFA liver contents remained unchanged between groups ($p > 0.05$).

In addition, Figure 6C presents the dimensionality reduction result using PCA of the liver FA composition per mice. The graph shows that the data from 6 mice per group (WT and SR-B1$^{-/-}$) are significantly different and can be independently clustered, supporting the result that the composition of the FA stored in the liver of both groups are different. Principal components 1 and 2 explained 66.5% of the liver FA composition variability (**Fig. 6C**).

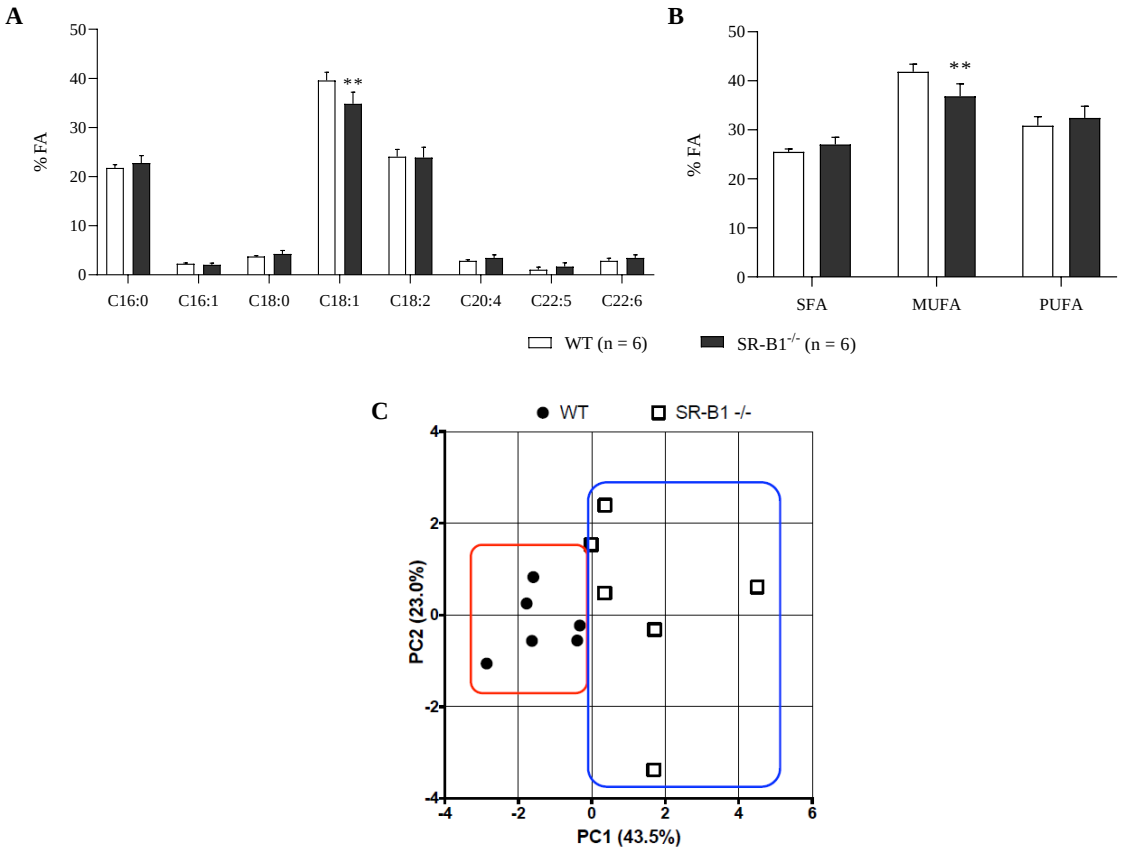

Fig 6. Liver FA composition in SR-B1$^{-/-}$ mice fed an HFD for 12 weeks. Percentage of (A) specific FA and **(B)** SFA, MUFA and PUFA content in livers of WT (n=6) and SR-B1$^{-/-}$ (n=6) mice. **(C)** Principal components analysis (PCA) for WT and SR-B1$^{-/-}$ obese mice. Data are shown as mean ± SD. * $p < 0.05$; ** $p < 0.01$ vs. WT mice.

9. DISCUSSION

Chronic overnutrition and sedentary lifestyles drive the epidemic of obesity in modern societies. Abnormalities in lipid and lipoprotein metabolism accompanied by chronic inflammation usually present in obese patients play an essential role in the development of several obesity-related comorbidities [36,37].

Even though SR-B1 is classically known for its role in HDL metabolism and CVD, new important functions in physiology and disease have been described for this receptor [38]. Here, we evaluated for the first time the impact of SR-B1 deficiency on adipocyte morphology, adipose tissue inflammation, and hepatic steatosis diet-induced obesity. In the present study, we demonstrated that the global deficiency of SR-B1 modifies the metabolic environment promoting an obesity phenotype characterized by inflammatory dyslipidemia associated with white adipocyte hypertrophy, increased adipose tissue macrophage infiltration, and attenuated hepatic steatosis in obese mice.

Obesity is intimately associated with dyslipidemia and atherosclerotic CVD. The hallmark of dyslipidemia in obesity is low HDL-C levels [39]. However, more recent evidence has demonstrated that cholesterol efflux capacity, more than HDL-C levels, is impaired in obese patients or mice, and is inversely associated with the incidence of cardiovascular events in a population-based cohort [40,41]. Indeed, SR-B1 knock-out mice are atherosclerosis prone despite exhibiting high HDL cholesterol levels (12-14). Interestingly, SR-B1-deficient HDL particles are abnormal in composition and function, which most likely lead to decreased anti-atherogenic activity (12-14). This HDL dysfunctionality together with the SR-B1-dependent pro-inflammatory profile observed in obese SR-B1$^{-/-}$ mice may significantly increase the risk of atherosclerosis. Thus, the mechanisms associated with

obesity and underlying compositional and functional HDL alterations are of substantial importance.

Curiously, previously published studies reported an association between some genetic variants in the human SR-B1 gene locus and the body mass index (BMI) [42,43]. Despite these human data, we did not observe any difference in murine body weight gain dependent of the SR-B1 genotype. However, it is essential to highlight that, despite that the major cause of obesity and its co-morbidities are related to abnormal food intake and body weight gain, some observations have documented that not all individuals become obese when consuming high-calorie diets [44]. Even in some studies, overweight and obese patients have shown a better prognosis than normal-weight subjects, suggesting that BMI is not always the best indicator of metabolic health [6].

Surprisingly, we found marked hypertriglyceridemia in SR-B1-deficient obese mice, compared to WT littermates. Based on combined data from prospective studies, TG levels are a risk factor for CVD, independent of HDL-C levels [45]. Adipose tissue has a central role in TG metabolism and proper WAT functionality is crucial for systemic metabolic homeostasis [27]. A recent observation indicates that cholesterol imbalance may contribute to adipocyte dysfunction and elevated blood TG levels in obese states [46]. Interestingly, abnormal cholesterol metabolism profoundly influences adipocyte homeostasis mimicking that found in hypertrophied adipocytes in obesity (46). An additional critical event in obesity is the macrophage infiltration of adipose tissue and macrophages resident within CLS in adipose tissue are lipid-laden and pro-inflammatory [47]. Data showed that apolipoprotein A-I (apoA-I), the major protein component of HDL particles, inhibits TLR4-mediated inflammatory signaling pathways in adipocytes by preventing MAPK and NF-κB activation via ATP-binding transmembrane transporters of the ABC family [48]. Considering that SR-B1 mRNA is highly expressed in differentiated

3T3 adipocytes and increases during differentiation [49], our data showing adipocyte hypertrophy and immune cell recruitment by CLS presence suggest that SR-B1 deficiency may contribute to the obesogenic environment by promoting higher circulating pro-inflammatory TNF-α and possibly by lowering anti-inflammatory IL-10 levels observed in these obese animals. In this regard, a substantial increase in SR-B1 protein expression was shown in 3T3 cells-derived adipocytes incubated with oxidized low-density lipoprotein (LDL), which prevented adipocyte inflammation [50]. On the other hand, interaction between SR-B1 and the sphingosine 1 phosphate (S1P) receptor modulates calcium flux in vitro [51]. Interestingly, intracellular calcium can modulate de novo lipogenesis and contribute to IR [52]. Since adipose tissue inflammation is a hallmark of central obesity and loss of adipocyte cholesterol efflux could directly contribute to systemic inflammation, our results reveal a close relationship between SR-B1 expression, nutrient excess, and activation of the immune system in eWAT. However, the precise role of SR-B1 in adipose tissue and glucose metabolism requires further investigation.

Subclinical low grade inflammation is induced by increased adiposity leading to significant co-morbidities in the liver, triggering a continuous vicious cycle [53]. The available evidence regarding the role of SR-B1 in the development of NAFLD is limited. A study showed that adult C57BL/6 mice fed with high fat and cholesterol diet increased hepatic mRNA and protein levels of SR-B1 in mice with NAFLD [54]. On the other hand, Pparg knockdown in mice improves fatty liver without alterations in Srebp1c mRNA levels [55], consistent with our results in mRNA levels of these genes in SR-B1-deficient obese animals. Furthermore, SR-B1 was involved hepatic VLDL remnant uptake in the absence of classical ApoE-recognizing receptors [56]. Also, less accumulation of MUFA in obese animals lacking SR-B1 suggests that the quality of FA accumulated in the liver, not only total fat content, may be critical to the progression and severity of NAFLD. Indeed, a high

hepatic MUFA (palmitoleic acid)/SFA (palmitic acid) ratio appears to be an indicator of more inflammatory NAFLD (34). Thus, reduced hepatic MUFA content in obese SR-B1$^{-/-}$ mice may indicate attenuated risk of developing more advanced liver disease. Remarkably, our data showed that SR-B1-deficient obese animals are also less prone to overall hepatic TG deposition, probably explained by dysregulation of transcription factors (Pparα and Pparγ) as well as lipid transport proteins (Cpt1 and Apob) that play a key role in FA catabolism and TG secretion. However, future studies evaluating the role of SR-B1 in hepatic inflammation and fibrosis in more advanced murine models of NAFLD are necessary.

A previous study have shown that supplementation with α-tocopherol/vitamin E, a potent lipid-soluble antioxidant, reduces adipose tissue inflammation and improves the overall metabolic profile in a mouse model of diet-induced obesity [57]. Moreover, vitamin E significantly improved liver function and histologic changes in patients with NAFLD [58]. These data are relevant, considering that our group previously demonstrated that vitamin E metabolism is abnormal in SR-B1-deficient mice [59]. Thus, SR-B1-dependent tissue α-tocopherol delivery may have also contributed to the WAT phenotype of obese SR-B1$^{-/-}$ mice.

Recently, an expert group suggested a new acronym (MAFLD, Metabolic Associated Fatty Liver Disease) for NAFLD that more accurately reflects current knowledge of fatty liver diseases associated with metabolic dysfunction [60]. Our data supports the hypothesis that variation in obesity phenotypes (e.g. systemic inflammation and liver fat accumulation) may be modulated by SR-B1 expression and function. Given the potentially opposite effects of SR-B1 expression on adipose tissue pathobiology versus fatty liver development, additional research to define more accurately the role of SR-B1 in a variety of metabolic diseases and different tissues are required.

Thus, one main limitation of our study is the use of an animal model with global SR-B1 deficiency, which makes it difficult to establish the tissue-specific (e.g., fat versus liver) role of SR-B1 expression during obesity. In addition, HFD intake for 12 weeks essentially promotes fatty liver, but it is not a good model to evaluate the relevance of SR-B1 function in further NASH progression (e.g. inflammation and/or fibrosis development). Such a study would likely need a larger sample size or narrower selection criteria.

10. CONCLUSION

We revealed liver and adipose tissue-specific disturbances underlying diet-induced obesity in SR-B1 deficiently mice. As potential implications of the current work, SR-B1 may be a therapeutic target not only in atherosclerotic CVD setting, but certainly also in obesity that increases chronic disease risk and mortality worldwide.

11. BIBLIOGRAPHY

[1] Obesity and overweight n.d. https://www.who.int/news-room/fact-sheets/detail/obesity-and-overweight (accessed December 10, 2019).

[2] Koliaki C, Liatis S, Kokkinos A. Obesity and cardiovascular disease: revisiting an old relationship. Metabolism 2019;92:98–107. https://doi.org/10.1016/j.metabol.2018.10.011.

[3] Polyzos SA, Kountouras J, Mantzoros CS. Obesity and nonalcoholic fatty liver disease: From pathophysiology to therapeutics. Metabolism 2019;92:82–97. https://doi.org/10.1016/j.metabol.2018.11.014.

[4] Gluchowski NL, Becuwe M, Walther TC, Farese R V. Lipid droplets and liver disease: From basic biology to clinical implications. Nat Rev Gastroenterol Hepatol 2017;14:343–55. https://doi.org/10.1038/nrgastro.2017.32.

[5] Younossi Z, Nasty QM, Marietti M, Hardy T, Henry L, Eslam M, et al. Global burden of NAFLD and NASH: Trends, predictions, risk factors and prevention. Nat Rev Gastroenterol Hepatol 2018;15:11–20. https://doi.org/10.1038/nrgastro.2017.109.

[6] Vecchié A, Dallegri F, Carbone F, Bonaventura A, Liberale L, Portincasa P, et al. Obesity phenotypes and their paradoxical association with cardiovascular diseases. Eur J Intern Med 2018;48:6–17. https://doi.org/10.1016/j.ejim.2017.10.020.

[7] Sookoian S, Pirola CJ, Valenti L, Davidson NO. Genetic pathways in nonalcoholic fatty liver disease: Insights from systems biology. Hepatology 2020:hep.31229. https://doi.org/10.1002/hep.31229.

[8] Choromanska B, Mysliwiec P, Hady HR, Dadan J, Mysliwiec H, Bonda T, et al. The implication of adipocyte ATP-binding cassette A1 and G1 transporters in metabolic

complications of obesity. J Physiol Pharmacol 2019;70. https://doi.org/10.26402/jpp.2019.1.14.

[9] Rao PK, Merath K, Drigalenko E, Jadhav AYL, Komorowski RA, Goldblatt MI, et al. Proteomic characterization of high-density lipoprotein particles in patients with non-alcoholic fatty liver disease. Clin Proteomics 2018;15:10. https://doi.org/10.1186/s12014-018-9186-0.

[10] Fan N, Peng L, Xia Z, Zhang L, Song Z, Wang Y, et al. Triglycerides to high-density lipoprotein cholesterol ratio as a surrogate for nonalcoholic fatty liver disease: A cross-sectional study. Lipids Health Dis 2019;18. https://doi.org/10.1186/s12944-019-0986-7.

[11] Fadaei R, Poustchi H, Meshkani R, Moradi N, Golmohammadi T, Merat S. Impaired HDL cholesterol efflux capacity in patients with non-alcoholic fatty liver disease is associated with subclinical atherosclerosis. Sci Rep 2018;8. https://doi.org/10.1038/s41598-018-29639-5.

[12] Rigotti A, Miettinen HE, Krieger M. The role of the high-density lipoprotein receptor SR-BI in the lipid metabolism of endocrine and other tissues. Endocr Rev 2003;24:357–87. https://doi.org/10.1210/er.2001-0037.

[13] Trigatti BL, Krieger M, Rigotti A. Influence of the HDL receptor SR-BI on lipoprotein metabolism and atherosclerosis. Arterioscler Thromb Vasc Biol 2003;23:1732–8. https://doi.org/10.1161/01.ATV.0000091363.28501.84.

[14] Leiva A, Verdejo H, Benítez ML, Martínez A, Busso D, Rigotti A. Mechanisms regulating hepatic SR-BI expression and their impact on HDL metabolism. Atherosclerosis 2011;217:299–307. https://doi.org/10.1016/j.atherosclerosis.2011.05.036.

[15] Dagher G, Donne N, Klein C, Ferré P, Dugail I. HDL-mediated cholesterol uptake and targeting to lipid droplets in adipocytes. J Lipid Res 2003;44:1811–20. https://doi.org/10.1194/jlr.M300267-JLR200.

[16] Yvan-Charvet L, Bobard A, Bossard P, Massiéra F, Rousset X, Ailhaud G, et al. In vivo evidence for a role of adipose tissue SR-BI in the nutritional and hormonal regulation of adiposity and cholesterol homeostasis. Arterioscler Thromb Vasc Biol 2007;27:1340–5. https://doi.org/10.1161/ATVBAHA.106.136382.

[17] Zhang Y, McGillicuddy FC, Hinkle CC, O'Neill S, Glick JM, Rothblat GH, et al. Adipocyte modulation of high-density lipoprotein cholesterol. Circulation 2010;121:1347–55. https://doi.org/10.1161/CIRCULATIONAHA.109.897330.

[18] Ahmed RAM, Murao K, Imachi H, Yu X, Li J, Wong NCW, et al. Human scavenger receptor class b type 1 is regulated by activators of peroxisome proliferators-activated receptor-γ in hepatocytes. Endocrine 2009;35:233–42. https://doi.org/10.1007/s12020-008-9142-2.

[19] Wang W, Yan Z, Hu J, Shen WJ, Azhar S, Kraemer FB. Scavenger receptor class B, type 1 facilitates cellular fatty acid uptake. Biochim Biophys Acta - Mol Cell Biol Lipids 2020;1865:158554. https://doi.org/10.1016/j.bbalip.2019.158554.

[20] Rivera K, Salas-Pérz F, Echeverría G, Urquiaga I, Dicenta S, Pérez D, et al. Red wine grape pomace attenuates atherosclerosis and myocardial damage and increases survival in association with improved plasma antioxidant activity in a murine model of lethal ischemic heart disease. Nutrients 2019;11. https://doi.org/10.3390/nu11092135.

[21] Folch J, Lees M, Sloane Stanley GH. A simple method for the isolation and purification of total lipides from animal tissues. J Biol Chem 1957;226:497–509. https://doi.org/10.3989/scimar.2005.69n187.

[22] Murano I, Barbatelli G, Parisani V, Latini C, Muzzonigro G, Castellucci M, et al. Dead adipocytes, detected as crown-like structures, are prevalent in visceral fat depots of genetically obese mice 2008. https://doi.org/10.1194/jlr.M800019-JLR200.

[23] Pfaffl MW. Relative expression software tool (REST(C)) for group-wise comparison and statistical analysis of relative expression results in real-time PCR. Nucleic Acids Res 2002;30:36e–36. https://doi.org/10.1093/nar/30.9.e36.

[24] Li X, Catalina F, Grundy SM, Patel S. Method to measure apolipoprotein B-48 and B-100 secretion rates in an individual mouse: Evidence for a very rapid turnover of VLDL and preferential removal of B-48- Relative to B-100-containing lipoproteins. J Lipid Res 1996;37:210–20.

[25] Xavier A, Zacconi F, Gainza C, Cabrera D, Arrese M, Uribe S, et al. Intrahepatic fatty acids composition as a biomarker of NAFLD progression from steatosis to NASH by using 1H-MRS. RSC Adv 2019;9:42132–9. https://doi.org/10.1039/c9ra08914d.

[26] Rigotti A, Trigatti BL, Penman M, Rayburn H, Herz J, Krieger M. A targeted mutation in the murine gene encoding the high density lipoprotein (HDL) receptor scavenger receptor class B type I reveals its key role in HDL metabolism. Proc Natl Acad Sci U S A 1997;94:12610–5. https://doi.org/10.1073/pnas.94.23.12610.

[27] Haczeyni F, Bell-Anderson KS, Farrell GC. Causes and mechanisms of adipocyte enlargement and adipose expansion. Obes Rev 2018;19:406–20. https://doi.org/10.1111/obr.12646.

[28] Longo M, Zatterale F, Naderi J, Parrillo L, Formisano P, Raciti GA, et al. Adipose tissue dysfunction as determinant of obesity-associated metabolic complications. Int J Mol Sci 2019;20. https://doi.org/10.3390/ijms20092358.

[29] Nimptsch K, Konigorski S, Pischon T. Diagnosis of obesity and use of obesity biomarkers in science and clinical medicine. Metabolism 2019;92:61–70. https://doi.org/10.1016/j.metabol.2018.12.006.

[30] Gan L, Xiang W, Xie B, Yu L. Molecular mechanisms of fatty liver in obesity. Front Med 2015;9:275–87. https://doi.org/10.1007/s11684-015-0410-2.

[31] Zhang YL, Hernandez-Ono A, Siri P, Weisberg S, Conlon D, Graham MJ, et al. Aberrant hepatic expression of PPARγ2 stimulates hepatic lipogenesis in a mouse model of obesity, insulin resistance, dyslipidemia, and hepatic steatosis. J Biol Chem 2006;281:37603–15. https://doi.org/10.1074/jbc.M604709200.

[32] de la Rosa Rodriguez MA, Kersten S. Regulation of lipid droplet-associated proteins by peroxisome proliferator-activated receptors. Biochim Biophys Acta - Mol Cell Biol Lipids 2017;1862:1212–20. https://doi.org/10.1016/j.bbalip.2017.07.007.

[33] Mittendorfer B, Yoshino M, Patterson BW, Klein S. VLDL triglyceride kinetics in lean, overweight, and obese men and women. J Clin Endocrinol Metab 2016;101:4151–60. https://doi.org/10.1210/jc.2016-1500.

[34] Yamada K, Mizukoshi E, Sunagozaka H, Arai K, Yamashita T, Takeshita Y, et al. Characteristics of hepatic fatty acid compositions in patients with nonalcoholic steatohepatitis. Liver Int 2015;35:582–90. https://doi.org/10.1111/liv.12685.

[35] de Souza CO, Teixeira AAS, Biondo LA, Lima Junior EA, Batatinha HAP, Rosa Neto JC. Palmitoleic acid improves metabolic functions in fatty liver by PPARα-dependent AMPK activation. J Cell Physiol 2017;232:2168–77. https://doi.org/10.1002/jcp.25715.

[36] Vekic J, Zeljkovic A, Stefanovic A, Jelic-Ivanovic Z, Spasojevic-Kalimanovska V. Obesity and dyslipidemia. Metabolism 2019;92:71–81. https://doi.org/10.1016/j.metabol.2018.11.005.

[37] Zhang T, Chen J, Tang X, Luo Q, Xu D, Yu B. Interaction between adipocytes and high-density lipoprotein:new insights into the mechanism of obesity-induced dyslipidemia and atherosclerosis. Lipids Health Dis 2019;18. https://doi.org/10.1186/s12944-019-1170-9.

[38] Hoekstra M, Sorci-Thomas M. Rediscovering scavenger receptor type BI: Surprising new roles for the HDL receptor. Curr Opin Lipidol 2017;28:255–60. https://doi.org/10.1097/MOL.0000000000000413.

[39] Lamon-Fava S, Wilson PWF, Schaefer EJ. Impact of body mass index on coronary heart disease risk factors in men and women: The Framingham Offspring Study. Arterioscler Thromb Vasc Biol 1996;16:1509–15. https://doi.org/10.1161/01.ATV.16.12.1509.

[40] Rohatgi A, Khera A, Berry JD, Givens EG, Ayers CR, Wedin KE, et al. HDL cholesterol efflux capacity and incident cardiovascular events. N Engl J Med 2014;371:2383–93. https://doi.org/10.1056/NEJMoa1409065.

[41] Duong MN, Uno K, Nankivell V, Bursill C, Nicholls SJ. Induction of obesity impairs reverse cholesterol transport in ob/ob mice. PLoS One 2018;13. https://doi.org/10.1371/journal.pone.0202102.

[42] Acton S, Osgood D, Donoghue M, Corella D, Pocovi M, Cenarro A, et al. Association of polymorphisms at the SR-BI gene locus with plasma lipid levels and body mass index in a white population. Arterioscler Thromb Vasc Biol 1999;19:1734–43. https://doi.org/10.1161/01.ATV.19.7.1734.

[43] Koumanis DJ, Christou N V., Wang XL, Gilfix BM. Pilot study examining the frequency of several gene polymorphisms in a morbidly obese population. Obes Surg 2002;12:759–64. https://doi.org/10.1381/096089202320995529.

[44] Cornier MA, Salzberg AK, Endly DC, Bessesen DH, Rojas DC, Tregellas JR. The effects of overfeeding on the neuronal response to visual food cues in thin and reduced-obese individuals. PLoS One 2009;4. https://doi.org/10.1371/journal.pone.0006310.

[45] Hokanson JE, Austin MA. Plasma triglyceride level is a risk factor for cardiovascular disease independent of high-density lipoprotein cholesterol level: A metaanalysis of population-based prospective studies. Eur J Cardiovasc Prev Rehabil 1996;3:213–9. https://doi.org/10.1177/174182679600300214.

[46] Yu B-L, Zhao S-P, Hu J-R. Cholesterol imbalance in adipocytes: a possible mechanism of adipocytes dysfunction in obesity. Obes Rev 2009;11:560–7. https://doi.org/10.1111/j.1467-789X.2009.00699.x.

[47] Ni Y, Ni L, Zhuge F, Xu L, Fu Z, Ota T. Adipose tissue macrophage phenotypes and characteristics: The key to insulin resistance in obesity and metabolic disorders. Obesity 2020;28:225–34. https://doi.org/10.1002/oby.22674.

[48] Sultana A, Cochran BJ, Tabet F, Patel M, Torres LC, Barter PJ, et al. Inhibition of inflammatory signaling pathways in 3T3-L1 adipocytes by apolipoprotein A-I. FASEB J 2016;30:2324–35. https://doi.org/10.1096/fj.201500026R.

[49] Acton SL, Scherer PE, Lodish HF, Krieger M. Expression cloning of SR-BI, a CD36-related class B scavenger receptor. J Biol Chem 1994;269:21003–9.

[50] Song G, Wu X, Zhang P, Yu Y, Yang M, Jiao P, et al. High-density lipoprotein inhibits ox-LDL-induced adipokine secretion by upregulating SR-BI expression and suppressing ER Stress pathway. Sci Rep 2016;6. https://doi.org/10.1038/srep30889.

[51] Lee MH, Appleton KM, El-Shewy HM, Sorci-Thomas MG, Thomas MJ, Lopes-Virella MF, et al. S1P in HDL promotes interaction between SR-BI and S1PR1 and

activates S1PR1-mediated biological functions: Calcium flux and S1PR1 internalization. J Lipid Res 2017;58:325–38. https://doi.org/10.1194/jlr.M070706.

[52] Wright LE, Vecellio Reane D, Milan G, Terrin A, Di Bello G, Belligoli A, et al. Increased mitochondrial calcium uniporter in adipocytes underlies mitochondrial alterations associated with insulin resistance. Am J Physiol - Endocrinol Metab 2017;313:E641–50. https://doi.org/10.1152/ajpendo.00143.2016.

[53] Cantero I, Abete I, Babio N, Arós F, Corella D, Estruch R, et al. Dietary Inflammatory Index and liver status in subjects with different adiposity levels within the PREDIMED trial. Clin Nutr 2018;37:1736–43. https://doi.org/10.1016/j.clnu.2017.06.027.

[54] Qiu Y, Liu S, Chen H-T, Yu C-H, Teng X-D, Yao H-T, et al. Upregulation of caveolin-1 and SR-B1 in mice with non-alcoholic fatty liver disease. Hepatobiliary Pancreat Dis Int 2013;12:630–6. https://doi.org/10.1016/S1499-3872(13)60099-5.

[55] Yamazaki T, Shiraishi S, Kishimoto K, Miura S, Ezaki O. An increase in liver PPARγ2 is an initial event to induce fatty liver in response to a diet high in butter: PPARγ2 knockdown improves fatty liver induced by high-saturated fat. J Nutr Biochem 2011;22:543–53. https://doi.org/10.1016/j.jnutbio.2010.04.009.

[56] Hu L, Van der Hoogt CC, Espirito Santo SMS, Out R, Kypreos KE, Van Vlijmen BJM, et al. The hepatic uptake of VLDL in lrp-ldlr-/-vldlr-/- mice is regulated by LPL activity and involves proteoglycans and SR-BI. J Lipid Res 2008;49:1553–61. https://doi.org/10.1194/jlr.M800130-JLR200.

[57] Alcalá M, Sánchez-Vera I, Sevillano J, Herrero L, Serra D, Ramos MP, et al. Vitamin E reduces adipose tissue fibrosis, inflammation, and oxidative stress and improves metabolic profile in obesity. Obesity 2015;23:1598–606. https://doi.org/10.1002/oby.21135.

[58] Sato K, Gosho M, Yamamoto T, Kobayashi Y, Ishii N, Ohashi T, et al. Vitamin E has a beneficial effect on nonalcoholic fatty liver disease: A meta-analysis of randomized controlled trials. Nutrition 2015;31:923–30. https://doi.org/10.1016/j.nut.2014.11.018.

[59] Mardones P, Strobel P, Miranda S, Leighton F, Quiñones V, Amigo L, et al. α-Tocopherol Metabolism Is Abnormal in Scavenger Receptor Class B Type I (SR-BI)-Deficient Mice. J Nutr 2002;132:443–9. https://doi.org/10.1093/jn/132.3.443

[60] Eslam M, Sanyal AJ, George J, Sanyal A, Neuschwander-Tetri B, Tiribelli C, et al. MAFLD: A consensus-driven proposed nomenclature for metabolic associated fatty liver fisease. Gastroenterology 2020;158:1999–2014.e1. https://doi.org/10.1053/j.gastro.2019.11.312. .